ACCOUNTS
of chemical research

Theory of Proton-Coupled Electron Transfer in Energy Conversion Processes

SHARON HAMMES-SCHIFFER*

Department of Chemistry, 104 Chemistry Building, Pennsylvania State University, University Park, Pennsylvania 16802

RECEIVED ON APRIL 22, 2009

Downloaded by PENNSYLVANIA STATE UNIV on October 23, 2009 | http://pubs.acs.org
Publication Date (Web): October 7, 2009 | doi: 10.1021/ar9001284

CONSPECTUS

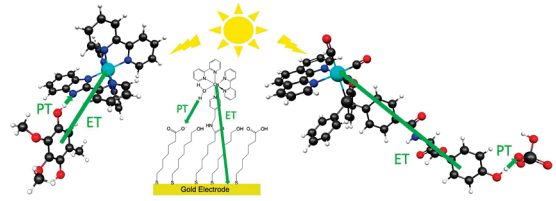

Proton-coupled electron transfer (PCET) reactions play an essential role in a broad range of energy conversion processes, including photosynthesis and respiration. These reactions also form the basis of many types of solar fuel cells and electrochemical devices. Recent advances in the theory of PCET enable the prediction of the impact of system properties on the reaction rates. These predictions may guide the design of more efficient catalysts for energy production, including those based on artificial photosynthesis and solar energy conversion. This Account summarizes the theoretically predicted dependence of PCET rates on system properties and illustrates potential approaches for tuning the reaction rates in chemical systems.

A general theoretical formulation for PCET reactions has been developed over the past decade. In this theory, PCET reactions are described in terms of nonadiabatic transitions between the reactant and product electron−proton vibronic states. A series of nonadiabatic rate constant expressions for both homogeneous and electrochemical PCET reactions have been derived in various well-defined limits. Recently this theory has been extended to include the effects of solvent dynamics and to describe ultrafast interfacial PCET. Analysis of the rate constant expressions provides insight into the underlying physical principles of PCET and enables the prediction of the dependence of the rates on the physical properties of the system. Moreover, the kinetic isotope effect, which is the ratio of the rates for hydrogen and deuterium, provides a useful mechanistic probe. Typically the PCET rate will increase as the electronic coupling and temperature increase and as the total reorganization energy and equilibrium proton donor−acceptor distance decrease. The rate constant is predicted to increase as the driving force becomes more negative, rather than exhibit turnover behavior in the inverted region, because excited vibronic product states associated with low free energy barriers and relatively large vibronic couplings become accessible. The physical basis for the experimentally observed pH dependence of PCET reactions has been debated in the literature. When the proton acceptor is a buffer species, the pH dependence may arise from the protonation equilibrium of the buffer. It could also arise from kinetic complexity of competing concerted and sequential PCET reaction pathways. In electrochemical PCET, the heterogeneous rate constants and current densities depend strongly on the overpotential. The change in equilibrium proton donor−acceptor distance upon electron transfer may lead to asymmetries in the Tafel plots and deviations of the transfer coefficient from the standard value of one-half at zero overpotential.

Applications of this theory to experimentally studied systems illustrate approaches that can be utilized to tune the PCET rate. For example, the rate can be tuned by changing the pH or using different buffer species as proton acceptors. The rate can also be tuned with site-specific mutagenesis in biological systems or chemical modifications that vary the substituents on the redox species in chemical systems. Understanding the impact of these changes on the PCET rate may assist experimental efforts to enhance energy conversion processes.

 © XXXX American Chemical Society

Introduction

The coupled transfer of electrons and protons underlies a broad range of energy conversion processes. Proton-coupled electron transfer (PCET) reactions[1−7] play an essential role in photosynthesis and respiration, as well as in many types of solar fuel cells and electrochemical devices. Thus, understanding the fundamental theoretical principles of PCET reactions is critical for the design of solar fuel cells and devices based on artificial photosynthesis. Recent advances in the theory of PCET enable the prediction of the impact of system properties on the reaction rates. These predictions may guide experimental efforts in tuning systems to enhance energy conversion processes.

This Account summarizes the theoretically predicted dependence of PCET rates on system properties and illustrates potential approaches for tuning the reaction rates in chemical systems. Here PCET reactions refer to the transfer of an electron and a proton in a single step without a stable intermediate. Such reactions are often denoted concerted, although the term concerted is not rigorously applicable because the electron and proton behave quantum mechanically and hence are delocalized. The PCET rate depends on the reorganization energy, the driving force, the electronic coupling, and the proton transfer interface properties, such as the equilibrium proton donor−acceptor distance and frequency. In addition to these properties that are directly related to the redox species, the PCET rate also depends on temperature, pH, overpotential in electrochemical processes, and solvent relaxation time in certain regimes.

Overview of PCET Theory

Typically PCET reactions are in the vibronically nonadiabatic regime because the couplings between the diabatic reactant and product vibronic states are significantly smaller than the thermal energy. In this regime, PCET reactions are described in terms of nonadiabatic transitions between the reactant and product electron−proton vibronic states.[2,6] The reactant electronic state corresponds to the electron localized on its donor, and the product electronic state corresponds to the electron localized on its acceptor. When the proton vibrational states are calculated for the proton potential energy curves associated with the reactant and product electronic states, the reactant and product electron−proton vibronic states are products of the corresponding electronic and proton vibrational states. In the limit of electronically nonadiabatic proton transfer, the coupling between a pair of vibronic states is the product of an electronic coupling and the overlap integral between the reactant and product proton vibrational wave functions.[7,8] In general, the overlap integral depends strongly on the proton donor−acceptor distance. As a result, the inclusion of the proton donor−acceptor vibrational motion is important for PCET reactions.[9]

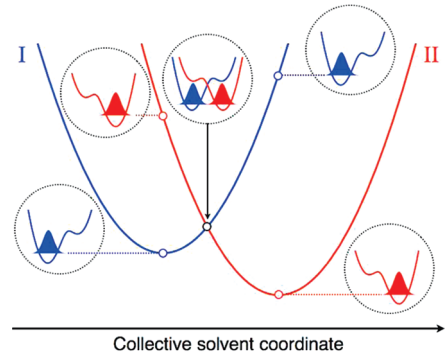

FIGURE 1. Slices of the free energy surfaces for the ground reactant (I) and product (II) vibronic states along a collective solvent coordinate. The proton potential energy curves and ground state proton vibrational wave functions with energies corresponding to open circles on the free energy curves are depicted. Reprinted from ref 6. Copyright 2008 American Chemical Society.

The fundamental mechanism of a typical PCET reaction is illustrated in Figure 1, which depicts slices of the ground state free energy surfaces along a collective solvent coordinate, in conjunction with the proton potential energy curves and the corresponding proton vibrational wave functions. As shown in this figure, the proton vibrational ground state wave function is localized near the donor for the reactant state and near the acceptor for the product state. Changes in the collective solvent coordinate (i.e., reorganization of the solvent environment) strongly impact the relative energies of the reactant and product proton potential energy curves. For a typical equilibrium PCET reaction, the system is initially at thermal equilibrium on the reactant surface, and fluctuations of the solvent environment bring the system to the crossing point between the two surfaces, where the reactant and product vibronic states are degenerate. The probability of a nonadiabatic transition from the reactant to the product surface is proportional to the square of the vibronic coupling, which in turn is proportional to the proton vibrational wave function overlap depicted in Figure 1. Subsequent to such a nonadiabatic transition, the system relaxes to thermal equilibrium on the product surface. In general, the excited vibronic states may also play an important role in PCET reactions.

We have derived a series of nonadiabatic rate constant expressions for PCET reactions in various well-defined limits.[6,9,10] These expressions are based on Fermi's golden rule formalism, which is valid in the vibronically nonadiabatic limit, in conjunction with linear response theory. The simplest rate constant expression is for fixed proton donor−acceptor

Downloaded by PENNSYLVANIA STATE UNIV on October 23, 2009 | http://pubs.acs.org
Publication Date (Web): October 7, 2009 | doi: 10.1021/ar9001284

Downloaded by PENNSYLVANIA STATE UNIV on October 23, 2009 | http://pubs.acs.org
Publication Date (Web): October 7, 2009 | doi: 10.1021/ar9001284

distance R and thus is valid for stiff hydrogen bonding interfaces. The more complete rate constant expression includes the motion of the R-mode, which is represented by a quantum mechanical harmonic oscillator associated with the reduced mass M and frequency Ω. We derived simplified versions of this rate constant expression in the low- and high-frequency regimes for the R-mode. The low-frequency (high-temperature) R-mode rate constant expression is based on the assumption that $\hbar\Omega \ll k_B T$, and the high-frequency (low-temperature) R-mode rate constant expression is based on the assumption that $\hbar\Omega \gg k_B T$.

The rate constant expression for fixed proton donor−acceptor distance R is[10]

$$k = \sum_{\mu} P_{\mu} \sum_{\nu} \frac{|V^{el} S_{\mu\nu}^{(0)}|^2}{\hbar} \sqrt{\frac{\pi}{\lambda_{\mu\nu} k_B T}} \exp\left[-\frac{(\Delta G_{\mu\nu}^0 + \lambda_{\mu\nu})^2}{4\lambda_{\mu\nu} k_B T}\right] \quad (1)$$

where the summations are over reactant and product vibronic states, P_μ is the Boltzmann probability for the reactant state μ, and V^{el} is the electronic coupling. In addition, $S_{\mu\nu}^{(0)}$ is the proton vibrational wave function overlap, $\lambda_{\mu\nu}$ is the total reorganization energy, and $\Delta G_{\mu\nu}^0$ is the free energy of reaction for vibronic states μ and ν. Often the reorganization energy $\lambda_{\mu\nu}$ is assumed to be the same for all pairs of states, and $\Delta G_{\mu\nu}^0$ is assumed to be the sum of the driving force $\Delta G^0 \equiv \Delta G_{00}^0$ and the difference between the product and reactant proton vibrational states relative to their respective ground states. When the proton donor−acceptor motion is included, the overlap is approximated as $S_{\mu\nu} = S_{\mu\nu}^{(0)} \exp[-\alpha_{\mu\nu}(R - \bar{R})]$, where $\bar{R}$ is the equilibrium value of R and $S_{\mu\nu}^{(0)}$ is the overlap at $R = \bar{R}$. The rate constant expression in the low-frequency (high-temperature) R-mode regime is similar to eq 1 but includes the extra prefactor $\exp[2k_B T\alpha_{\mu\nu}^2/M\Omega^2]$, and the total reorganization energy includes two additional terms due to the dependence of the vibronic coupling on R and the reorganization energy corresponding to the R-mode. The rate constant expression in the high-frequency (low-temperature) R-mode regime is similar to eq 1 but includes an extra prefactor that depends on the frequency Ω but not on the temperature.

The form of the rate constant in eq 1 is valid for vibronically nonadiabatic reactions, where the solvent time scale is much faster than the time scale associated with nonadiabatic transitions between vibronic states. The specific form of the vibronic coupling in eq 1 is valid for electronically nonadiabatic proton transfer, where the proton tunneling time scale is significantly faster than the electronic transition time scale.[7,8] In the opposite regime of electronically adiabatic proton transfer (e.g., traditional hydrogen atom transfer),[8] the vibronic coupling is no longer the product of the electronic coupling and the proton vibrational wave function overlap.

The kinetic isotope effect (KIE), which is the ratio of the rate for hydrogen to the rate for deuterium, provides a useful mechanistic probe for PCET reactions. Based on the rate constant given in eq 1 and related expressions, the KIE is proportional to the ratio of the overlaps of the hydrogen and deuterium vibrational wave functions for a given pair of reactant/product vibronic states. Typically this ratio of overlaps increases as the overlaps decrease. Thus, this ratio is larger for greater proton donor−acceptor distances and is smaller for excited vibronic states than for the ground vibronic states because the excited state proton vibrational wave functions are more delocalized. The magnitude of the KIE has been observed experimentally to range from moderate (e.g., 2−3) to extremely large (e.g., >50).[4,11] As will be discussed below, analysis of the magnitude and temperature dependence of the KIE provides insight into the underlying PCET mechanism.

We have also extended this theoretical formulation to electrochemical PCET.[12−14] Specifically, we have derived expressions for the heterogeneous rate constants and current densities for processes in which proton transfer occurs within a solvated hydrogen-bonded solute complex concurrently with electron transfer between the solute complex and the immersed electrode. The resulting expressions for the transition probabilities are similar to those derived for homogeneous PCET with the reaction free energy replaced by an expression that depends on the energy of the one-electron acceptor state in the electrode, the potential at the redox species in solution due to the electrical double layer formed by the supporting electrolyte ions, and the overpotential. The heterogeneous rate constant expressions are obtained by integration over the energy levels in the conduction band of the electrode, weighting the transition probability according to the Fermi distribution and the density of states of the electrode. The anodic and cathodic current densities are obtained by integrating the product of the rate constant and the relevant solute complex concentration over the distance between the solute complex and the electrode surface.

Recently we have extended the theory of PCET beyond the golden rule formalism and derived rate constant expressions that include the effects of solvent dynamics in both homogeneous and electrochemical PCET.[15] These expressions interpolate between the golden rule and solvent-controlled limits, where the golden rule limit is defined in terms of weak vibronic coupling and fast solvent relaxation, and the solvent-controlled limit is defined in terms of strong vibronic coupling and slow solvent relaxation.[16,17] In both cases, the overall

Downloaded by PENNSYLVANIA STATE UNIV on October 23, 2009 | http://pubs.acs.org
Publication Date (Web): October 7, 2009 | doi: 10.1021/ar9001284

treatment is nonadiabatic in the sense that transitions between electronic states are involved. Consistent with our previous work, the rate constant is proportional to the square of the vibronic coupling and is independent of the solvent relaxation time in the golden rule limit. In contrast, the rate constant is independent of the vibronic coupling and increases as the solvent relaxation time decreases in the solvent-controlled limit. The interconversion between these two limits can be induced by altering the proton transfer interface properties (i.e., the proton donor−acceptor mode frequency and the proton vibrational wave function overlap), the electronic coupling, the solvent relaxation time, and the overpotential in the case of electrochemical PCET.

Moreover, the KIE behaves differently in the golden rule and solvent-controlled limits and thus provides a unique probe for distinguishing between these two different regimes. As discussed above, the KIE can be quite large in the golden rule limit because it is approximately proportional to the square of the ratio of the overlaps of the hydrogen and deuterium vibrational wave functions. The KIE is expected to be more moderate in the solvent-controlled limit because it arises mainly from differences in zero-point energy and vibronic energy level splitting.

Dependence of PCET Rates on System Properties

Analysis of the rate constant expressions described above provides insight into the underlying physical principles of PCET and enables the prediction of the dependence of the rates on physical properties of the system. In general, the PCET rate will increase as the electronic coupling increases and as the total reorganization energy decreases. In the solvent-controlled limit defined above, the PCET rate will increase as the solvent relaxation time decreases. The dependence of the PCET rate on the proton transfer interface properties, driving force, temperature, pH, and electrochemical potential is more complicated and will be discussed in the remainder of this section.

The rates of PCET reactions are strongly influenced by the properties of the proton transfer interface. The rate increases dramatically as the equilibrium proton donor−acceptor distance decreases due to the increase in the proton vibrational wave function overlap. Furthermore, typically the rate increases as the proton donor−acceptor mode frequency decreases because the lower frequency enables sampling of smaller distances corresponding to larger overlaps. This effect is evident in the prefactor $\exp[2k_BT\alpha_{\mu\nu}^2/M\Omega^2]$ that arises in the low-frequency *R*-mode regime. Often the proton donor−acceptor mode frequency decreases as the equilibrium distance increases, so these two trends may work against each other when designing proton transfer interfaces aimed at enhancing the PCET rate.

The KIE is also strongly influenced by the proton transfer interface properties. As mentioned in the previous section, the KIE is approximately proportional to the square of the ratio of the hydrogen and deuterium vibrational wave-function overlaps. For a given pair of reactant/product vibronic states, the KIE increases as the equilibrium proton donor−acceptor distance increases when all other parameters remain the same. Moreover, in the low-frequency *R*-mode regime, the KIE increases as the proton donor−acceptor mode frequency increases due to the prefactor mentioned above. Again, these two trends may work against each other because the proton donor−acceptor mode frequency often decreases as the equilibrium distance increases.

In addition, the rates of PCET reactions depend strongly on the driving force.[18] On the basis of eq 1 with only the ground vibronic states included, the rate constant would exhibit a turnover as ΔG^0 becomes more negative, with a maximum at $-\Delta G^0 = \lambda$, as depicted by the dashed line in Figure 2a. This turnover is similar to the inverted region turnover predicted by Marcus theory for electron transfer.[19] As indicated by the solid line in Figure 2a, however, the inclusion of excited vibronic states leads to qualitatively different behavior. In particular, the rate constant will increase as ΔG^0 becomes more negative because excited vibronic product states associated with low free energy barriers and relatively large vibronic couplings become accessible. The PCET rate constant will eventually decrease for highly exoergic reactions that are expected to be experimentally inaccessible. Note that ET reactions coupled to low-frequency vibrational modes can exhibit an inverted region turnover at experimentally accessible driving forces. This behavior is not predicted for PCET reactions mainly because of the high frequency of the proton vibrational motion, as well as the greater shift of the proton vibrational wave function.[38]

Moreover, the excited vibronic states also impact the qualitative behavior of the driving force dependence of the KIE. The ln(KIE) exhibits a very weak quadratic dependence on driving force, with a maximum at $\Delta G^0 \approx 0$, when only the ground states are included. In contrast, the ln(KIE) decreases much more rapidly for both positive and negative driving forces when excited vibronic states are included because the contributions from excited vibronic states increase as the reaction becomes more asymmetric, and contributions from excited vibronic states decrease the KIE. These trends are illustrated in Figure 2b and are further clarified in Figure 2c, which

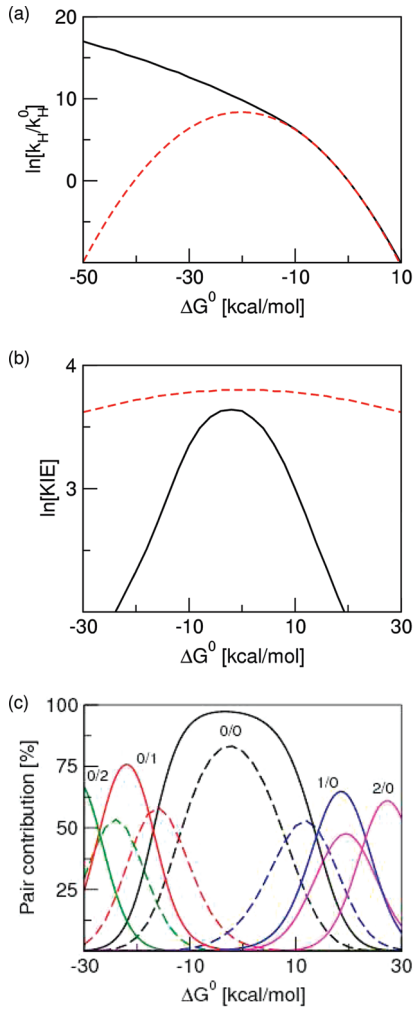

FIGURE 2. Driving force dependence of (a) the rate constant in the low-frequency *R*-mode regime, (b) the associated KIE, and (c) the contributions of pairs of reactant/product vibronic states for a model system. In panels a and b, the dashed red curve corresponds to the calculation including only the ground reactant and product vibronic states, and the solid black curve corresponds to the calculation converged with respect to excited vibronic states. In panel c, the color code for pairs of reactant/product vibronic states is as follows: 0/0 (black), 1/0 (blue), 2/0 (magenta), 0/1 (red), and 0/2 (green). Reprinted from ref 18. Copyright 2009 American Chemical Society.

illustrates that the (0/0) pair dominates at $\Delta G^0 \approx 0$, whereas other pairs dominate sequentially as the reaction becomes more endergonic or exergonic.

Similar to most chemical reactions, PCET rates increase with temperature. The temperature dependence of the rate is dictated mainly by the exponential term in eq 1, which typically overrides the temperature-dependent prefactor. Because of contributions from excited vibronic states, the increase of the rate with temperature may not behave as a single exponential. Moreover, in the low-frequency *R*-mode regime, the additional temperature-dependent exponential term also increases with temperature.

The KIE, however, can exhibit more interesting temperature dependence. The temperature dependence of the KIE has been measured experimentally to probe the detailed mechanism of PCET reactions.[11,20] Assuming that the driving force and reorganization energy are independent of isotope and only the ground states contribute to the overall rate, the rate constant expression in eq 1 for fixed *R* predicts that the KIE will be independent of temperature. Using the same assumptions in the low-frequency *R*-mode regime, the KIE is predicted to decrease with temperature as $\exp[-2k_BT(\alpha_D^2 - \alpha_H^2)/M\Omega^2]$, where $\alpha_D > \alpha_H$ because the overlap decreases faster with *R* for deuterium than for hydrogen. This factor tends to dominate the temperature dependence of the KIE in the low-frequency *R*-mode regime even when excited vibronic states are involved. Since this temperature-dependent factor is not present in the high-frequency *R*-mode regime, however, the KIE could either increase or decrease with temperature in this regime when excited vibronic states contribute significantly to the overall rate.

A number of experimental studies have illustrated that the rate of PCET reactions depends strongly on pH. The basis for this pH dependence has been discussed extensively in the literature.[21−26] When the proton acceptor is a buffer species in solution, the pH dependence is thought to arise from the protonation equilibrium of the buffer.[21,22] The pH dependence of tyrosine oxidation for one specific ruthenium−polypyridyl−tyrosine system has been observed to be independent of the buffer, however, and has been interpreted in terms of proton transfer to bulk water.[21,23] The physical basis for the pH dependence observed in this system is not fully resolved.[24−26] In general, the pH dependence of PCET reactions could arise from the kinetic complexity of competing concerted and sequential PCET reaction pathways,[25,26] as well as pathways involving different proton acceptors, including various buffer species and hydroxide. Moreover, the pH dependence could be caused by the impact of pH on the physical properties of the proton transfer interface, such as hydrogen bond strength, proton donor−acceptor distance, and frequencies. Experimental verification of these hypotheses is challenging.

In electrochemical PCET, the heterogeneous rate constants and current densities depend strongly on the electrode potential. Similar to homogeneous PCET, the current densities also depend on the proton transfer interface properties, reorganization energy, temperature, and pH. In addition, the effective activation energies associated with the current densities of

Downloaded by PENNSYLVANIA STATE UNIV on October 23, 2009 | http://pubs.acs.org
Publication Date (Web): October 7, 2009 | doi: 10.1021/ar9001284

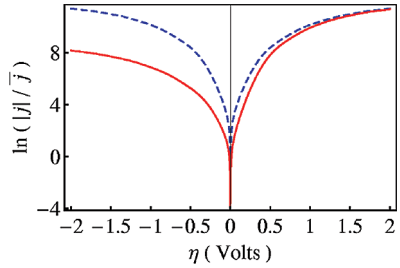

FIGURE 3. Logarithm of the scaled current density as a function of overpotential for a model electrochemical PCET system. The solid red and dashed blue curves correspond to $\delta R = 0.05$ Å and $\delta R = 0$, respectively. Reprinted from ref 6. Copyright 2008 American Chemical Society.

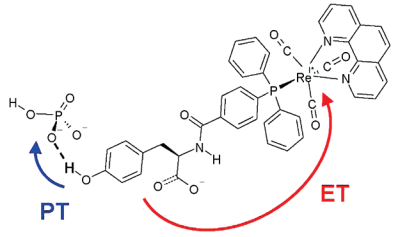

FIGURE 4. PCET reaction induced by photoexcitation of the rhenium−tyrosine complex[27] to a metal-to-ligand charge transfer state. The proton transfers to a hydrogen-bonded phosphate HPO_4^{2-} buffer. Reprinted from ref 28. Copyright 2007 American Chemical Society.

electrochemical PCET reactions contain temperature-dependent terms arising from the change in the equilibrium proton donor−acceptor distance upon electron transfer. This term has a different sign for the cathodic and anodic processes, leading to asymmetries of the Tafel plots, which depict the dependence of current density on overpotential, even for small changes in the equilibrium proton donor−acceptor distance.[12] Figure 3 depicts the Tafel plot for a model electrochemical PCET system with a change in the equilibrium proton donor−acceptor distance of $\delta R = 0.05$ Å upon oxidation. In addition to causing asymmetry in the Tafel plot, the change in the equilibrium proton donor−acceptor distance upon electron transfer also causes the transfer coefficient to deviate from the standard value of one-half at zero overpotential.

Tuning Chemical PCET Systems

PCET in the tyrosine-bound rhenium−polypyridyl complex shown in Figure 4 has been studied experimentally by photoexcitation to the metal-to-ligand charge transfer excited state.[21,27] The rate constant was found to increase with pH in the presence of phosphate buffer and to be independent of pH in the absence of phosphate buffer in the range $4 < pH < 8$. Moreover, the rate constant was found to be independent of phosphate buffer concentration at low pH, where the dominant buffer species is $H_2PO_4^-$. These experimental data suggest that the reaction occurs by a PCET mechanism in which the electron transfers from the tyrosine to the rhenium while the proton transfers from the tyrosine to the phosphate buffer species HPO_4^{2-} but not to $H_2PO_4^-$.

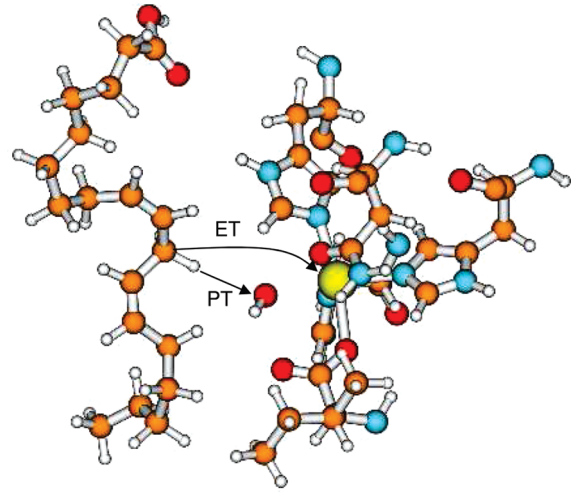

FIGURE 5. The hydrogen abstraction step of the reaction catalyzed by soybean lipoxygenase with linoleic acid substrate. Reprinted from ref 30. Copyright 2007 American Chemical Society.

We modeled the pH dependence of the overall rate for this rhenium system in terms of a titration between the HPO_4^{2-} and $H_2PO_4^-$ forms of the phosphate buffer.[28] In this case, the overall rate constant is the sum of the unimolecular electron transfer rate constant and the bimolecular PCET rate constant weighted by the concentration of HPO_4^{2-}.[21] Analysis of the PCET calculations provided insight into the interplay among the reorganization energy, reaction free energy, and vibronic coupling for this system. The excited product vibronic states were found to contribute significantly to the overall rate. For these types of systems, in which the proton acceptor is a buffer species, the overall rate constant can be tuned by changing the pH or using different buffer species.

Activation of the C−H bond in linoleic acid by the enzyme soybean lipoxygenase has been studied experimentally.[11] As depicted in Figure 5, this reaction is thought to occur by a PCET mechanism, in which the electron transfers from the π-system of the substrate to the iron of the cofactor, while the proton transfers from a substrate carbon atom to the hydroxyl ligand of the cofactor. The KIE was observed to be 81 at room temperature and to decrease weakly with temperature.[11] Our calculations indicated that the unusually large magnitude of the KIE arises from the relatively small proton vibrational wave function overlap and the dominance of the ground vibronic states in the tunneling process.[29,30] Since the proton is transferred between a carbon and an oxygen atom, the hydrogen bond is relatively weak, and the system is in the low-fre-

Downloaded by PENNSYLVANIA STATE UNIV on October 23, 2009 | http://pubs.acs.org
Publication Date (Web): October 7, 2009 | doi: 10.1021/ar9001284

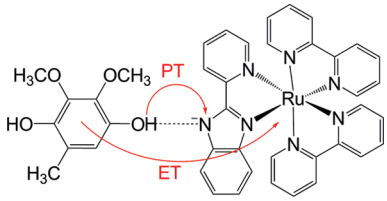

FIGURE 6. PCET reaction corresponding to oxidation of UQH_2 following photoexcitation of the ruthenium−bipyridyl complex to a metal-to-ligand charge transfer state. Reprinted from ref 34. Copyright 2009 American Chemical Society.

quency proton donor−acceptor mode regime. As discussed above, in this regime the temperature dependence of the KIE is dominated by a factor that decays exponentially with temperature, consistent with the experimentally observed trend.

Mutation of Ile553, which is bordering the linoleic acid substrate but is ~15 Å from the iron atom, was observed experimentally to impact the KIE for soybean lipoxygenase.[11,31,32] According to the experimental data, as residue 553 becomes less bulky, the magnitude and temperature dependence of the KIE increases. Modeling of these kinetic data indicates that, as residue 553 becomes less bulky, the proton donor−acceptor equilibrium distance increases and the frequency decreases.[31,32] For these types of biological systems, the PCET rate can be tuned by altering the properties of the proton transfer interface through site-specific mutagenesis.

Quinol oxidation in the biomimetic model system depicted in Figure 6 has been studied experimentally in acetonitrile by photoexcitation to a metal-to-ligand charge transfer state, which induces electron transfer from the quinol to the ruthenium concurrent with proton transfer from the quinol to the ligand nitrogen.[20] The average KIEs at 296 K were measured to be 1.87 and 3.45 for ubiquinol (UQH_2) and plastoquinol (PQH_2) analogues, respectively, and the KIE was found to increase with temperature for UQH_2 but decrease with temperature for PQH_2. The increase in KIE with increasing temperature (i.e., the greater apparent activation free energy for hydrogen than for deuterium) is unusual in the context of most semiclassical models based on transition state theory. Similar behavior was observed for quinol oxidation reactions in the cytochrome *bc*1 complex and in ethanol.[20,33]

Our calculations provide a plausible explanation for the differences in magnitudes and temperature dependences of the KIEs for the two quinol systems and, in particular, an explanation for the unusual inverse temperature dependence of the KIE for UQH_2.[34] The hydrogen bonds for these quinol systems were found to be stiff, and the systems were determined to be in the high-frequency proton donor−acceptor regime. In this regime, the rate constant may be approximated by the fixed proton donor−acceptor distance expression given in eq 1, and

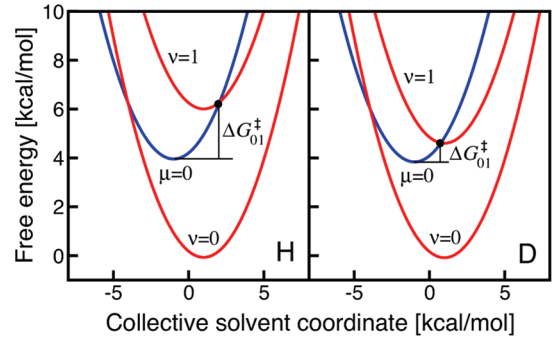

FIGURE 7. Free energy curves as functions of a collective solvent coordinate for the UQH_2 system. The lowest energy reactant vibronic state ($\mu = 0$) and lowest two product vibronic states (μ=0, 1) are shown for H (left) and D (right). All states are shifted so the lowest energy reactant vibronic state has zero energy for both H and D. The free energy barrier for the (0/1) pair of reactant/product vibronic states is smaller for D than for H because of the smaller vibronic energy level splittings for D. Reprinted from ref 34. Copyright 2009 American Chemical Society.

the temperature dependence of the KIE is not dominated by the temperature-dependent pre-exponential factor that was dominant for the lipoxygenase system.

The physical explanation of the inverse temperature dependence of the KIE for the UQH_2 system is illustrated in Figure 7. The inverse temperature dependence of the KIE may be observed if the (0/0) pair of reactant/product vibronic states is in the inverted Marcus region, while the (0/1) pair of reactant/product vibronic states is in the normal Marcus region and is the dominant contributor to the overall rate. The inverted Marcus region for the (0/0) pair of vibronic states is defined as $-\Delta G^0 > \lambda$, which is typically accessible for relatively small reorganization energies. Figure 7 indicates that the free energy barriers for the UQH_2 system are similar for the (0/0) and (0/1) pairs of vibronic states. The (0/1) pair of vibronic states is the dominant contributor for this system because of the greater vibronic coupling (i.e., proton vibrational wave function overlap). In this case, the temperature dependence of the KIE is determined mainly by the factor $\exp[-(\Delta G_{01}^{\ddagger}(H) - \Delta G_{01}^{\ddagger}(D))/k_B T]$, which will increase as the temperature increases when $\Delta G_{01}^{\ddagger}(H) > \Delta G_{01}^{\ddagger}(D)$. As illustrated in Figure 7, the free energy barrier for the dominant transition is lower for deuterium than for hydrogen because of the smaller splittings between the vibronic energy levels for deuterium. As a result, the KIE increases with increasing temperature for the UQH_2 system.

The qualitatively different behavior for the two quinol systems is due to the rather subtle differences in the driving forces and the proton potential energy curves, which impact the free energy barriers and vibronic couplings for each pair of reactant/product vibronic states and thereby determine the relative contributions from each pair. In the PQH_2 system,

Downloaded by PENNSYLVANIA STATE UNIV on October 23, 2009 | http://pubs.acs.org
Publication Date (Web): October 7, 2009 | doi: 10.1021/ar9001284

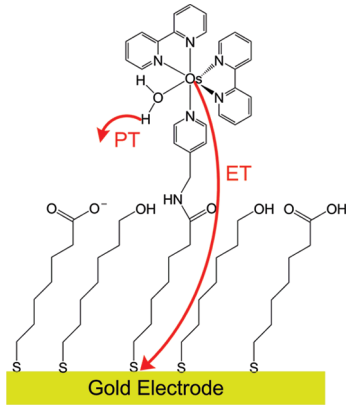

FIGURE 8. Electrochemical PCET reaction for a system comprised of an osmium−bipyridyl−aquo complex attached to a mixed self-assembled monolayer on a gold electrode. The proton acceptor has been proposed to be a carboxylate group of the monolayer.[36]

other pairs of reactant/product vibronic states contribute significantly to the overall rate, leading to more complex temperature dependence of the KIE and an overall decrease in the KIE with increasing temperature. Note that the UQH_2 and PQH_2 analogues differ only with respect to the OCH_3 and CH_3 substituents on the quinol. For these types of quinol systems, the PCET rate can be tuned by altering the driving force and the proton potential energy curves with varying substituents.

The PCET reaction in a system comprised of an osmium aquo complex attached to a mixed self-assembled monolayer on a gold electrode, as depicted in Figure 8, has been studied experimentally.[35] Cyclic voltammetry was used to examine the kinetics of the PCET reaction in both H_2O and D_2O for different chain lengths at various pH values. The rate constant was observed to be highly sensitive to the chain length, and the KIE was ~2 over a wide range of pH values. The experimental data were also used to generate plots of the transfer coefficient α_{PCET} and the logarithm of the rate as a function of the overpotential η. The transfer coefficient was observed to be ~0.46 at $\eta = 0$, and the Tafel plot was observed to be asymmetric.

Our theoretical formulation of electrochemical PCET provides an explanation for these observations.[12] As discussed above, the asymmetry of the Tafel plot is predicted by the theory due to the additional term in the effective activation energy with a different sign for the cathodic and anodic processes. This term is proportional to δR, which is the difference between the equilibrium proton donor−acceptor distance for the oxidized and reduced osmium complex. In addition, the theory predicts that the transfer coefficient at $\eta = 0$ can be estimated as $0.5 - \alpha_{00}\delta R\, k_B T/\Lambda_{00}$, where Λ_{00} is the total reorganization energy defined in ref 12. Calculations on models for the osmium system with a carboxylate group acting as the proton acceptor[36] indicate that $\delta R \approx 0.17$ Å, and physically reasonable values of the other parameters suggest that the calculated transfer coefficient will be in a range that is consistent with the experimental measurement. For electrochemical PCET systems, chemical modifications that alter the relative proton donor−acceptor distance in the oxidized and reduced molecular species will impact the Tafel plot and the transfer coefficient.

Concluding Remarks

The PCET theory described in this Account provides predictions of the behavior of reaction rates with respect to system properties, including reorganization energy, driving force, proton transfer interface distances and frequencies, temperature, pH, solvent relaxation time, and overpotential. While some of these predictions have been shown to be consistent with experimental data, other predictions still await experimental validation. Recently we have extended this theory to describe photoinduced homogeneous PCET reactions and ultrafast interfacial PCET processes, which have been studied experimentally for a system comprised of methanol adsorbed on a titanium dioxide surface.[37] These theoretical developments, in conjunction with continual feedback between experiment and theory, will assist in guiding the design of more efficient catalysts for energy conversion processes.

I am grateful to Alexander Soudackov, Michelle Ludlow, Sarah Edwards, and Charulatha Venkataraman for helpful discussions and creation of the figures. This work was supported by NSF Grant No. CHE-07-49646, NSF Grant No. CHE-0802907 for POWERING THE PLANET: A Chemical Bonding Center, and NIH Grant No. GM56207.

BIOGRAPHICAL INFORMATION

Sharon Hammes-Schiffer received her B.A. from Princeton University in 1988 and her Ph.D. from Stanford University in 1993. Subsequently, she spent two years at AT&T Bell Laboratories as a postdoctoral research scientist. In 1995, she accepted a position as the Clare Boothe Luce Assistant Professor of Chemistry and Biochemistry at the University of Notre Dame. She moved to The Pennsylvania State University as the Shaffer Associate Professor of Chemistry in 2000, was promoted to Professor of Chemistry in 2003, and was appointed the Eberly Professor of Biotechnology in 2006. She has been a Senior Editor for *The Journal of Physical Chemistry* since 2001. Her research centers on the theoretical and computational investigation of proton, hydride, and proton-coupled electron transfer reactions in chemical and biological processes.

FOOTNOTES

*E-mail: shs@chem.psu.edu.

Downloaded by PENNSYLVANIA STATE UNIV on October 23, 2009 | http://pubs.acs.org
Publication Date (Web): October 7, 2009 | doi: 10.1021/ar9001284

Downloaded by PENNSYLVANIA STATE UNIV on October 23, 2009 | http://pubs.acs.org
Publication Date (Web): October 7, 2009 | doi: 10.1021/ar9001284

REFERENCES

1 Cukier, R. I.; Nocera, D. G. Proton-coupled electron transfer. *Annu. Rev. Phys. Chem.* **1998**, *49*, 337–369.

2 Hammes-Schiffer, S. Theoretical perspectives on proton-coupled electron transfer reactions. *Acc. Chem. Res.* **2001**, *34*, 273–281.

3 Mayer, J. M. Proton-coupled electron transfer: A reaction chemist's view. *Annu. Rev. Phys. Chem.* **2004**, *55*, 363–390.

4 Huynh, M. H.; Meyer, T. J. Proton-coupled electron transfer. *Chem. Rev.* **2007**, *107*, 5004–5064.

5 Rosenthal, J.; Nocera, D. G. Role of proton-coupled electron transfer in O−O bond activation. *Acc. Chem. Res.* **2007**, *40*, 543–553.

6 Hammes-Schiffer, S.; Soudackov, A. V. Proton-coupled electron transfer in solution, proteins, and electrochemistry. *J. Phys. Chem. B* **2008**, *112*, 14108–14123.

7 Georgievskii, Y.; Stuchebrukhov, A. A. Concerted electron and proton transfer: Transition from nonadiabatic to adiabatic proton tunneling. *J. Chem. Phys.* **2000**, *113*, 10438–10450.

8 Skone, J. H.; Soudackov, A. V.; Hammes-Schiffer, S. Calculation of vibronic couplings for phenoxyl/phenol and benzyl/toluene self-exchange reactions: Implications for proton-coupled electron transfer mechanisms. *J. Am. Chem. Soc.* **2006**, *128*, 16655–16663.

9 Soudackov, A.; Hatcher, E.; Hammes-Schiffer, S. Quantum and dynamical effects of proton donor−acceptor vibrational motion in nonadiabatic proton-coupled electron transfer reactions. *J. Chem. Phys.* **2005**, *122*, 014505.

10 Soudackov, A.; Hammes-Schiffer, S. Derivation of rate expressions for nonadiabatic proton-coupled electron transfer reactions in solution. *J. Chem. Phys.* **2000**, *113*, 2385–2396.

11 Knapp, M. J.; Rickert, K. W.; Klinman, J. P. Temperature dependent isotope effects in soybean lipoxygenase-1: Correlating hydrogen tunneling with protein dynamics. *J. Am. Chem. Soc.* **2002**, *124*, 3865–3874.

12 Venkataraman, C.; Soudackov, A. V.; Hammes-Schiffer, S. Theoretical formulation of nonadiabatic electrochemical proton-coupled electron transfer at metal-solution interfaces. *J. Phys. Chem. C* **2008**, *112*, 12386–12397.

13 Navrotskaya, I.; Soudackov, A. V.; Hammes-Schiffer, S. Model system-bath Hamiltonian and nonadiabatic rate constants for proton-coupled electron transfer at electrode-solution interfaces. *J. Chem. Phys.* **2008**, *128*, 244712.

14 Costentin, C. Electrochemical approach to the mechanistic study of proton-coupled electron transfer. *Chem. Rev.* **2009**, *108*, 2145–2179.

15 Navrotskaya, I.; Hammes-Schiffer, S. Electrochemical proton-coupled electron transfer: Beyond the golden rule. *J. Chem. Phys.* **2009**, *131*, 024112.

16 Zusman, L. D. Outer-sphere electron transfer in polar solvents. *Chem. Phys.* **1980**, *49*, 295–304.

17 Sparpaglione, M.; Mukamel, S. Dielectric friction and the transition from adiabatic to nonadiabatic electron transfer I. Solvation dynamics in Liouville space. *J. Chem. Phys.* **1988**, *88*, 3263–3280.

18 Edwards, S. J.; Soudackov, A. V.; Hammes-Schiffer, S. Analysis of kinetic isotope effects for proton-coupled electron transfer reactions. *J. Phys. Chem. A* **2009**, *113*, 2117–2126.

19 Marcus, R. A. Relation between charge transfer absorption and fluorescence spectra and the inverted region. *J. Chem. Phys.* **1989**, *93*, 3078–3086.

20 Cape, J. L.; Bowman, M. K.; Kramer, D. M. Reaction intermediates of quinol oxidation in a photoactivatable system that mimics electron transfer in the cytochrome bc1 complex. *J. Am. Chem. Soc.* **2005**, *127*, 4208–4215.

21 Irebo, T.; Reece, S. Y.; Sjodin, M.; Nocera, D. G.; Hammarstrom, L. Proton-coupled electron transfer of tyrosine oxidation: Buffer dependence and parallel mechanisms. *J. Am. Chem. Soc.* **2007**, *129*, 15462–15464.

22 Fecenko, C. J.; Meyer, T. J.; Thorp, H. H. Electrocatalytic oxidation of tyrosine by parallel rate-limiting proton transfer and multistate electron-proton transfer. *J. Am. Chem. Soc.* **2006**, *128*, 11020–11021.

23 Sjodin, M.; Styring, S.; Akermark, B.; Sun, L.; Hammarstrom, L. Proton-coupled electron transfer from tyrosine in a tyrosine-ruthenium-tris-bipyridine complex: Comparison with tyrosinez oxidation in photosystem II. *J. Am. Chem. Soc.* **2000**, *122*, 3932–3936.

24 Krishtalik, L. I. pH-dependent redox potential: how to use it correctly in the activation energy analysis. *Biochim. Biophys. Acta* **2003**, *1604*, 13–21.

25 Costentin, C.; Robert, M.; Saveant, J.-M. Concerted proton-electron transfer reactions in water: Are the driving force and rate constant depending on pH when water acts as a proton donor or acceptor. *J. Am. Chem. Soc.* **2007**, *129*, 5870–5879.

26 Finklea, H. O. Theory of coupled electron-proton transfer with potential-dependent transfer coefficients for redox couples attached to electrodes. *J. Phys. Chem. B* **2001**, *105*, 8685–8693.

27 Reece, S. Y.; Nocera, D. G. Direct tyrosine oxidation using the MLCT excited states of rhenium polypyridyl complexes. *J. Am. Chem. Soc.* **2005**, *127*, 9448–9458.

28 Ishikita, H.; Soudackov, A. V.; Hammes-Schiffer, S. Buffer-assisted proton-coupled electron transfer in a model rhenium-tyrosine complex. *J. Am. Chem. Soc.* **2007**, *129*, 11146–11152.

29 Hatcher, E.; Soudackov, A. V.; Hammes-Schiffer, S. Proton-coupled electron transfer in soybean lipoxygenase. *J. Am. Chem. Soc.* **2004**, *126*, 5763–5775.

30 Hatcher, E.; Soudackov, A. V.; Hammes-Schiffer, S. Proton-coupled electron transfer in soybean lipoxygenase: Dynamical behavior and temperature dependence of kinetic isotope effects. *J. Am. Chem. Soc.* **2007**, *129*, 187–196.

31 Meyer, M. P.; Klinman, J. P. Modeling temperature dependent kinetic isotope effects for hydrogen transfer in a series of soybean lipoxygenase mutants: The effect of anharmonicity upon transfer distance. *Chem. Phys.* **2005**, *319*, 283–296.

32 Meyer, M. P.; Tomchick, D. R.; Klinman, J. P. Enzyme structure and dynamics affect hydrogen tunneling: The impact of a remote side chain (I553) in soybean lipoxygenase-1. *Proc. Natl. Acad. Sci. U.S.A.* **2008**, *105*, 1146–1151.

33 Nagaoka, S.-i.; Inoue, M.; Nishioka, C.; Nishioku, Y.; Tsunoda, S.; Ohguchi, C.; Ohara, K.; Mukai, K.; Nagashima, U. Tunneling effect in antioxidant, prooxidant, and regeneration reactions of vitamin E. *J. Phys. Chem. B* **2000**, *104*, 856–862.

34 Ludlow, M. K.; Soudackov, A. V.; Hammes-Schiffer, S. Theoretical analysis of the unusual temperature dependence of the kinetic isotope effect in quinol oxidation. *J. Am. Chem. Soc.* **2009**, *131*, 7094–7102.

35 Madhiri, N.; Finklea, H. O. Potential-, pH-, and isotope-dependence of proton-coupled electron transfer of an osmium aquo complex attached to an electrode. *Langmuir* **2006**, *22*, 10643–10651.

36 Costentin, C.; Robert, M.; Saveant, J.-M.; Teillout, A.-L. Concerted and stepwise proton-coupled electron transfers in aquo/hydroxo complex couples in water: Oxidative electrochemistry of $[Os^{II}(bpy)_2(py)(OH_2)]^{2+}$. *ChemPhysChem* **2009**, *10*, 191–198.

37 Li, B.; Zhao, J.; Onda, K.; Jordan, K. D.; Yang, J.; Petek, H. Ultrafast proton-coupled electron transfer. *Science* **2006**, *311*, 1436–1440.

38 Edwards, S. J.; Soudackov, A. V.; Hammes-Schiffer, S. Driving force dependence of rates for nonadiabatic proton and proton-coupled electron transfer: Conditions for inverted region behavior. *J. Phys. Chem. B.* **2009**, in press, DOI: 10.1021/jp907808t.